
JOURNAL OF THE AMERICAN CHEMICAL SOCIETY

Long-Range Guanine Damage in Single-Stranded DNA: Charge Transport through a Duplex Bridge and in a Single-Stranded Overhang

Yongzhi Kan and Gary B. Schuster*

Contribution from the School of Chemistry and Biochemistry, Georgia Institute of Technology, Atlanta, Georgia 30332

Received June 28, 1999

Abstract: A series of anthraquinone-linked DNA oligonucleotides was prepared to examine the migration and reactions of radical cations in duplex and single-stranded regions. There are fewer nucleotides in the strand complementary to the AQ-containing strand, which creates a duplex with an overhang. This complementary strand contains three GG steps, which serve as traps for the radical cation. One GG step is in the duplex region, a second is adjacent to the duplex, and the third is in the single-strand overhang. Irradiation at 350 nm excites the anthraquinone and results in radical cation injection into the duplex DNA region. Treatment of the irradiated sample with piperidine or with formamidopyrimidine glycosylase results in strand cleavage that is detected by polyacrylamide gel electrophoresis and autoradiography. The pattern of reactivity at the three GG steps was examined for various oligonucleotide sequences. These studies confirm that the products of radical cation reaction differ in single-strand and duplex regions with 7,8-dihydro-8-oxo-guanine predominating in the latter. The results show that the radical cation can migrate from the duplex region onto the single strand. Radical cation transport in the single-strand overhang is proposed to proceed from guanine to guanine by means of direct contact in GG mispairs.

Introduction

Long-distance radical cation migration in DNA is a focus of intense scrutiny because it causes damage at guanines, which results in mutations^{1,2} and because of interest in the mechanism of the charge migration.^{3,4} Migration of radical cations from a point of origin near an electron acceptor covalently linked to DNA to a remote GG or GGG step (the electron donor) has

been demonstrated definitively.⁵⁻⁹ For some time, there was disagreement about the mechanism of migration,¹⁰⁻¹⁶ but recent experimental results are leading to a growing consensus that

(1) Burrows, C. J.; Muller, J. G. *Chem. Rev.* **1998**, *98*, 1109-1154.
(2) LePage, F.; Guy, A.; Cadet, J.; Sarasin, A.; Gentil, A. *Nucleic Acids Res.* **1998**, *26*, 1276-1281.
(3) Turro, N. J.; Barton, J. K. *J. Biol. Inorg. Chem.* **1998**, *3*, 201-209.
(4) Beratan, D. N.; Priyadarshy, S.; Risser, S. M. *Chem. Biol.* **1997**, *4*, 3-8.
(5) Arkin, M. R.; Stemp, E. D.; Pulver, S. C.; Barton, J. K. *Chem. Biol.* **1997**, *4*, 389-400.

(6) Hall, D. B.; Holmlin, R. E.; Barton, J. K. *Nature* **1996**, *382*, 731-735.

(7) Gasper, S. M.; Schuster, G. B. *J. Am. Chem. Soc.* **1997**, *119*, 12762-12771.

(8) Nunez, M.; Hall, D. B.; Barton, J. K. *Chem. Biol.* **1999**, *6*, 85-97.

(9) Meggers, E.; Michel-Beyerle, M. E.; Giese, B. *J. Am. Chem. Soc.* **1998**, *120*, 12950-12995.

(10) Kelley, O. S.; Barton, J. K. *Chem. Biol.* **1998**, *5*, 413-425.

(11) Brun, A. M.; Harriman, A. *J. Am. Chem. Soc.* **1992**, *114*, 3656-3660.

(12) Meade, T. J.; Kayyem, J. F. *Angew. Chem., Int. Ed. Engl.* **1995**, *34*, 352-354.

(13) Lewis, F. D.; Wu, T.; Zhang, Y.; Letsinger, R. L.; Greenfield, S. R.; Wasielewski, M. R. *Science* **1997**, *277*, 673-676.

the rate and efficiency of charge transport are controlled by local DNA structural dynamics.^{17,18} DNA is most commonly encountered as its canonical double helix, but it also has the ability to form other ordered structures such as hairpins, triplexes, and quadruplexes^{19,20} and disordered structures composed of single-stranded coils. We have undertaken an investigation of the migration and reactions of radical cations injected into these diverse DNA structures.

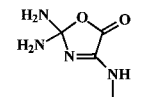
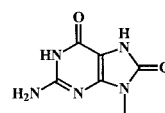
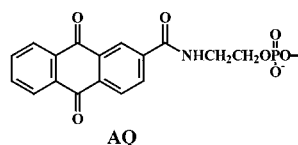
There are a few reports of studies designed to probe radical cation migration from a neighboring base to a guanine in single-stranded DNA. Candeias and Steenken²¹ examined oxidation of dinucleoside phosphates in solution and found rapid migration to guanine. Melvin, O'Neill, and co-workers²² used pulsed laser irradiation at 193 nm to ionize single-stranded oligonucleotides. They concluded that radical cation migration occurs between certain neighboring bases. Most recently, Giese and co-workers reported that radical cation migration in single-stranded DNA has a more shallow distance dependence than in duplex structures.²³ This is attributed to the flexibility of single-stranded structures. One objective of the experiments we report here is to address systematically questions of efficiency and mechanism for radical cation migration in single-strand DNA.

The products formed from the reaction of a guanine radical cation apparently depend on whether it is in a free nucleoside or part of a duplex. Cadet and co-workers report that 7,8-dihydro-8-oxo-guanine (8-OxoG) is a predominant product of riboflavin-sensitized oxidation or high-intensity laser photolysis of guanines in duplex DNA,^{24,25} but that this reaction gives 2,2-diaminoxazolone when a free guanosine derivative is oxidized.²⁶ Ito and co-workers reported²⁷ that riboflavin-sensitization of duplex DNA gives strand cleavage selectively at the 5'-G of GG steps with formation of 8-OxoG. Similarly, Saito and co-workers²⁸ first reported that sensitization of the hexameric duplex 5'-TTGGTA-3' gives selective 5'-G cleavage. However, most recently Saito and Sugiyama report²⁹ that the same hexamer gives equal cleavage at 3'- and 5'-G of the GG step and that oxazolone, not 8-OxoG, is the major product. A second objective of the experiments we report here is to identify systematically the products formed from guanine radical cations in single-strand and duplex DNA.

We recently developed a simple technique for covalently coupling a tethered anthraquinone derivative (AQ, see Chart 1) to a 5'-terminus of DNA oligonucleotides.⁷ Covalent attachment

Chart 1. Structure of DNA, DNA Conjugates, and Oxidation Products

Og12	5'-CGCGTTACCTTT-3'
DNA(1)	3'-GCGCAATGG ₁ AAATGG ₂ AAATATGG ₃ CTAAG-5'
DNA(2)	5'-CGCGTTACCTTTACCTTATACCGATTC-3'
DNA(3)	5'-ACCTTATACCGATTC-3'
DNA(4)	3'-GCGCAATGG ₁ AAATGG ₂ AAATATGG ₃ CTAAG-5'
DNA(5)	3'-GCGCAATGG ₁ AAATGG ₂ TTTTGG ₃ TTTT-5'
DNA(6)	3'-GCGCAATGG ₁ AAAGGG ₂ AAATATGG ₃ CTAAG-5'
DNA(7)	3'-GCGCAATGG ₁ AAATATGG ₂ ATAAGGG ₃ CTAAG-5'
DNA(8)	3'-GCGCAATGG ₁ AAATATAATATGG ₃ CTAAG-5'
DNA(8c)	5'-ATATTATACCGATTC-3'



defines the AQ location and restricts its allowable interaction geometries with DNA. In particular, we have shown that the four-atom tether of AQ that links the quinone group to the terminal phosphate is too short to permit intercalation. Chemical, spectroscopic, and modeling data indicate that the anthraquinone is associated (end-capped) with the terminal base pair of the oligonucleotide due primarily to stabilizing hydrophobic interactions.^{7,30} Irradiation of the end-capped quinone leads to one-electron oxidation of a neighboring DNA base to form its radical cation. Migration of the radical cation through the DNA duplex is revealed by reactions at remote GG steps that are assayed by measuring strand cleavage of radiolabeled samples caused by treatment with piperidine or by reaction catalyzed with formamidopyrimidine glycosylase (Fpg).³¹

We analyzed the chemical reactions of a series of AQ-linked DNA systems, which contain both duplex and single-stranded regions. These experiments provide information on radical cation migration through a duplex DNA bridge to and along a single strand of DNA. Measurements of reaction efficiency and product analysis show that radical cation migration occurs in the single-strand structure. The mechanism of charge transport in the single strand differs from that found in duplex B-form DNA.

Results

(1) Preparation and Characterization of AQ-Conjugates.

One challenge associated with investigation of radical cation transport in a disordered structure is to devise a system that permits identification of a starting point for the migration. Our approach employs a duplex DNA structure, AQ-Og12/DNA-(1), having a covalently linked AQ at one end and a single strand "overhang" at the other. DNA(1), the sequences are shown in Chart 1, contains three GG steps. GG₁ is located in the duplex

(29) Kino, K.; Saito, I.; Sugiyama, H. *J. Am. Chem. Soc.* **1998**, *120*, 7373–7374.

(30) Guckian, K. M.; Schweitzer, B. A.; Ren, R.; X.-F.; Sheils, C. J.; Paris, P. L.; Tahmassebi, D. C.; Kool, E. T. *J. Am. Chem. Soc.* **1996**, *118*, 8182–8183.

(31) Krokan, H. E.; Standal, R.; Slupphaug, G. *Biochem. J.* **1997**, *325*, 1–16.

(14) Fukui, K.; Tanaka, K. *Angew. Chem., Int. Ed.* **1998**, *37*, 158–161.
 (15) Jortner, J.; Bixon, M.; Langenbacher, T.; Michel-Beyerle, M. E. *Proc. Natl. Acad. Sci. U.S.A.* **1998**, *95*, 12759–12765.
 (16) Ratner, M. *Nature* **1999**, *397*, 480–481.
 (17) Wan, C.; Fiebig, T.; Kelley, S. O.; Treadway, C. R.; Barton, J. K.; Zewail, A. H. *Proc. Natl. Acad. Sci. U.S.A.* **1999**, *96*, 6014–6019.
 (18) Henderson, P. T.; Jones, D.; Hampikian, G.; Kan, Y.; Schuster, G. B. *Proc. Natl. Acad. Sci. U.S.A.* **1999**, *96*, 8353–8358.
 (19) Kang, C.; Zhang, X.; Ratliff, R.; Moyzis, R.; Rich, A. *Nature* **1992**, *356*, 126–131.
 (20) Sundquist, W. I.; Kliu, A. *Nature* **1989**, *342*, 825–829.
 (21) Candeias, L. P.; Steenken, S. *J. Am. Chem. Soc.* **1993**, *115*, 2437–2440.
 (22) Melvin, T.; Botchway, S.; Parker, A. W.; O'Neill, P. *J. Chem. Soc. Chem. Commun.* **1995**, 653–654.
 (23) Meggers, E.; Kusch, D.; Spichty, M.; Wille, U.; Giese, B. *Angew. Chem., Int. Ed.* **1998**, *37*, 459–462.
 (24) Kasai, H.; Yamaizumi, Z.; Berger, M.; Cadet, J. *J. Am. Chem. Soc.* **1992**, *114*, 9692–9694.
 (25) Angelov, D.; Spassky, A.; Berger, M.; Cadet, J. *J. Am. Chem. Soc.* **1997**, *119*, 11373–11380.
 (26) Cadet, J.; Berger, M.; Buchko, G. W.; Joshi, P. C.; Raoul, S.; Ravanat, J.-L. *J. Am. Chem. Soc.* **1994**, *116*, 7403–7404.
 (27) Ito, K.; Inoue, S.; Yamamoto, K.; Kawanishi, S. *J. Biol. Chem.* **1993**, *268*, 13221–13227.
 (28) Saito, I.; Takayama, M.; Sugiyama, H.; Nakatani, K.; Tsuchida, A.; Yamamoto, M. *J. Am. Chem. Soc.* **1995**, *117*, 6406–6407.

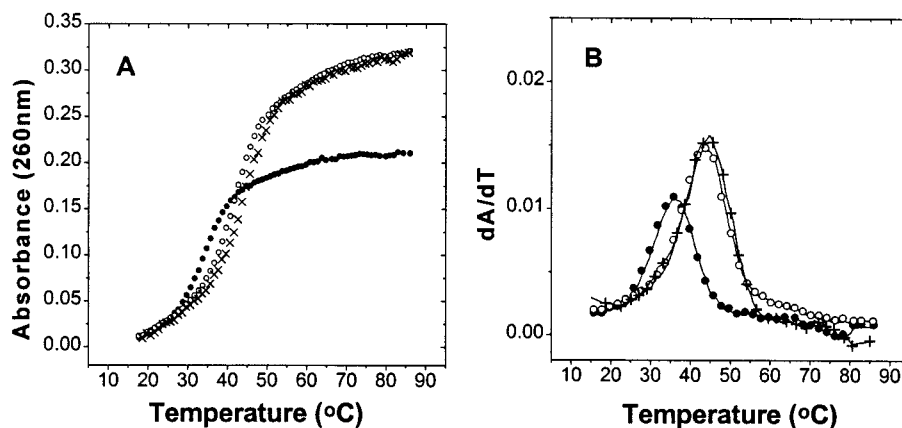


Figure 1. A. Melting curves monitored at 260 nm: (●) Og12/DNA(1), $T_m = 35$ °C; (○) DNA(1)/DNA(2), $T_m = 44$ °C; (×) AQ-Og12/DNA(1), $T_m = 44$ °C. The reduced absorbance change seen for Og12/DNA(1) may be due to incomplete duplex formation at 20 °C. B. First derivative plots of melting curves shown in A.

region formed by DNA(1) and its partial complement AQ-Og12. GG₂ is located one base into the overhang region, and GG₃ is eight bases away from the end of the duplex region of Og12 and is thus at least 40 Å (3.4 Å/base pair) away from GG₂. This compound affords a well-defined location for radical cation generation, provides a structured duplex region for its transport, and has three unique GG steps to probe radical cation migration and reactions.

We have shown previously that UV irradiation of anthraquinones intercalated or covalently bound to DNA leads to rapid electron-transfer resulting in the quinone radical anion and a base radical cation.^{32–35} The radical anion is quenched by molecular oxygen, and the radical cation migrates through duplex DNA leading to selective reaction predominantly at the 5'-G of GG steps. In AQ-Og12/DNA(1), GG₁ is the first GG step the radical cation will encounter. Reaction (assayed as strand cleavage) at this site provides a standard for comparison with reactions at GG₂ and GG₃. DNA(3) is the complement to the overhang region of DNA(1). The three-part structure [AQ-Og12+DNA(3)]/DNA(1) places all three GG steps in duplex regions. Comparison of the products formed by irradiation of AQ-Og12/DNA(1) with those formed from [AQ-Og12+DNA(3)]/DNA(1) permits isolation of the differences between GG steps in duplex and single-strand regions.

The oligonucleotides depicted in Chart 1 were synthesized by standard solid-phase methods, purified by HPLC, characterized using spectroscopic methods and by sequencing using the Maxam–Gilbert reactions.³⁶ The properties of the DNA duplexes and their interaction with the AQ were investigated by thermal denaturation experiments monitored by UV absorption at 260 nm, Figure 1. These experiments show smooth transitions for AQ-Og12/DNA(1) and for the compound lacking the quinone, Og12/DNA(1). The melting curves show only one well-defined transition, but this result does not eliminate the possibility of secondary structure in the single-strand overhang region where hypochromicity changes may be small. The observed T_m for AQ-Og12/DNA(1) is 44 °C, which is 10 °C greater than

for Og12/DNA(1) and thus reveals the significant stabilizing effect of the quinone expected from the end-capping model.

(2) Photoinduced GG Oxidative Damage. The effect of irradiation (350 nm, 20 °C) of the quinone in AQ-Og12/DNA(1) was examined with 5'-radiolabeled DNA(1) by polyacrylamide gel electrophoresis (PAGE) and autoradiography. After irradiation, but before analysis, excess DNA(2), a complete complement to DNA(1), was added to each sample and hybridized by heating to 90 °C followed by slow cooling to room temperature to form the DNA(1)/DNA(2) duplex. This ensures that each GG step in DNA(1) will respond uniformly to subsequent treatment. These samples were treated with piperidine (90 °C, 30 min) to reveal alkaline labile sites. The results of the PAGE autoradiogram are shown in Figure 2.

As expected, irradiation of AQ-Og12/DNA(1) leads to cleavage at GG₁, located in the duplex region, predominantly at the 5'-G (lane 3). Surprisingly, strand cleavage is also observed in the single-strand region at GG₂ and GG₃; however, in these cases the 5'- and 3'-G are cleaved with approximately equal efficiency. Figure 2, lane 6, shows results from irradiation of [AQ-Og12+DNA(3)]/DNA(1). Importantly in this "full duplex" (there is a nick between AQ-Og12 and DNA(3)), 5'-G-selective cleavage is seen at each of the GG-steps including GG₂ and GG₃. Clearly, irradiation of these AQ-conjugated DNA systems initiates reaction at guanines in both duplex and single-strand regions that are a considerable distance from the quinone. Further, the characteristic 5'-selective cleavage seen for GG steps in duplex DNA^{6,27,28,34} is absent when the GG step is in the single-stranded region.

Long-distance reactions such as those described above may be intramolecular or intermolecular. We performed a series of control experiments to assess the manner of reaction for this case. A possible route for intermolecular long-distance reaction involves singlet oxygen (¹O₂), which might be formed from the triplet state of the quinone. Singlet oxygen is a diffusible species that is known to react nonselectively with guanines in DNA yielding products that cause strand cleavage when treated with piperidine.^{37–39} The involvement of ¹O₂ was assessed by changing the solvent from H₂O to D₂O and by specifically generating ¹O₂ with methylene blue (MB).^{40,41} It is well-known that the lifetime of ¹O₂ is ~10-fold longer in D₂O than in H₂O

(32) Armitage, B. A.; Yu, C.; Devadoss, C.; Schuster, G. B. *J. Am. Chem. Soc.* **1994**, *116*, 9847–9859.

(33) Breslin, D. T.; Schuster, G. B. *J. Am. Chem. Soc.* **1996**, *118*, 2311–2319.

(34) Ly, D.; Kan, Y.; Armitage, B.; Schuster, G. B. *J. Am. Chem. Soc.* **1996**, *118*, 8747–8748.

(35) Gasper, S. M.; Schuster, G. B. *J. Am. Chem. Soc.* **1997**, *119*, 12762–12771.

(36) Maxam, A. M.; Gilbert, W. *Nucleic Acids, Pt. I. In Methods in Enzymology*; Academic Press: New York, 1980; Vol. 5.

(37) Blazek, E. R.; Peak, J. G.; Peak, M. J. *Photochem. Photobiol.* **1989**, *49*, 607–613.

(38) Floyd, R. A.; West, M. S.; Eneff, K. L.; Schneider, J. E. *Archiv. Biochem. Biophys.* **1989**, *273*, 106–111.

(39) Devasagayam, T. P. A.; Steenken, S.; Obendorf, M. S. W.; Schulz, W. A.; Sies, H. *Biochemistry* **1991**, *30*, 6283–6289.

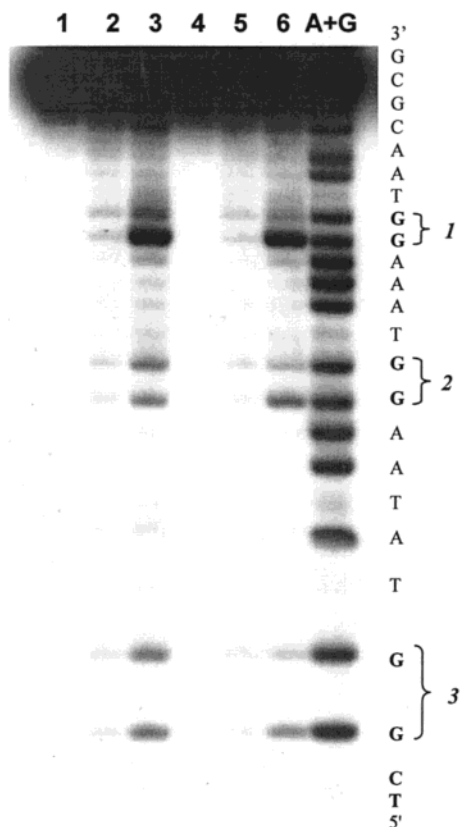


Figure 2. Autoradiogram depicting light-induced cleavage of GG₁, GG₂, and GG₃ in DNA(1)/AQ-Og12 and in DNA(1)/[AQ-Og12+DNA(3)] duplexes (4 μ M). Irradiation times are in parentheses. All lanes are piperidine treated. Lane 1: DNA(1)/AQ-Og12, dark control (0 min); lane 2: DNA(1)/Og12, light control (60 min); lane 3: DNA(1)/AQ-Og12 (60 min); lane 4: DNA(1)/[AQ-Og12+DNA(3)], dark control (0 min); lane 5: DNA(1)/[Og12+DNA(3)], light control (60 min); lane 6: DNA(1)/[AQ-Og12+DNA(3)] (60 min). A+G Maxam–Gilbert A+G sequencing lane. DNA(1) is ³²P 5'-end labeled.

and that this causes increased reaction efficiency in D₂O. Figure 3 shows an autoradiogram from experiments with AQ-Og12/DNA(1) carried out in H₂O and D₂O. There is no measurable solvent isotope effect. However, as expected, there is an easily observed isotope effect in the cleavage efficiency when the reaction of ¹O₂ with AQ-Og12/DNA(1) is sensitized with MB. These experiments show that ¹O₂ does not play a consequential role in the reactions at guanine, initiated by irradiation of the anthraquinone in AQ-Og12/DNA(1). A second control experiment was designed to probe the possibility that intermolecular association between DNA molecules in solution causes the apparent long-distance reaction at the guanines. Irradiation of a mixture containing 4 μ M of unlabeled AQ-Og12/DNA(1) and 4 μ M of a ³²P-labeled noncomplementary, GG-containing oligonucleotide (either as a single strand or as a duplex) reveals no cleavage in the noncomplementary strand. These experiments show that the long-distance reaction of AQ-Og12/DNA(1) is intramolecular. The injected radical cation migrates through the duplex and into the single strand leading to reactions at the GG steps.

(3) Sequence Effects on Guanine Reactions in Single-Strand DNA. Selective reaction at GG steps and, to a lesser extent, at 5'-GA-3' steps is a hallmark of radical cation reactions

(40) Rogers, M. A. J.; Snowden, P. T. *J. Am. Chem. Soc.* **1982**, *104*, 5541–5543.

(41) Showen, K. B.; Showen, R. L. *Solvent Isotope Effects on Enzyme Systems*; Academic Press: New York, 1982; Vol. 87.

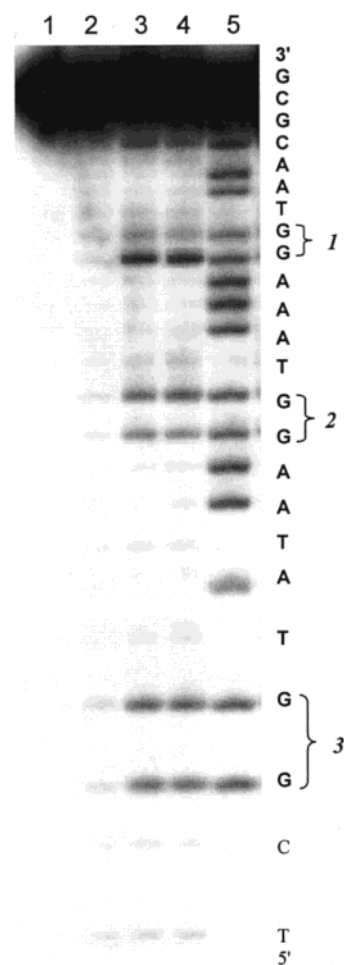


Figure 3. Autoradiogram depicting the effect of deuterated water (D₂O) on the photocleavage of DNA(1). All lanes are piperidine treated. Lane 1: DNA(1)/AQ-Og12, dark control; lane 2: DNA(1)/Og12, light control (60 min); lane 3: DNA(1)/AQ-Og12, H₂O (60 min); lane 4: DNA(1)/AQ-Og12, D₂O (60 min); lane 5: Maxam–Gilbert A+G sequencing. DNA(1) is ³²P 5'-end labeled.

in duplex DNA. Compared with guanines in GG steps, isolated guanines (that is, a G- not 5'- to a G or an A) are essentially unreactive.³² We examined the photochemistry of AQ-Og12/DNA(4) to probe the relative reactivity of GG steps and isolated guanines in single-strand DNA. DNA(4) is identical to DNA(1) except that GG₃ is replaced by 5'-GT-3'. Figure 4 shows the results of irradiation of AQ-Og12/DNA(4) followed by piperidine treatment. Strand cleavage is readily detected at the isolated guanine, which is 21 bases from the AQ. A control experiment shows that there is no detectable cleavage at this isolated G when the single-strand region is hybridized with its complementary strand. This result demonstrates that the operational reaction mechanisms in the single-strand region and in the duplex region are different.

The data in Figure 2 show that the efficiencies of cleavage at GG₂ and GG₃ are approximately the same—a finding that confirms relative distance independence in single-stranded DNA reported by Giese for a different system.²³ In contrast, the efficiency of radical cation reactions in duplex DNA falls off exponentially with migration distance.^{8,18} The mechanism of radical cation transport in the single-strand region was examined in more detail by further modification to the sequence of bases. For example, the AATATT sequence in DNA(1) between GG₂ and GG₃ was changed to (T)₅ in DNA(5). The results of irradiation of AQ-Og12/DNA(5) are shown schematically in

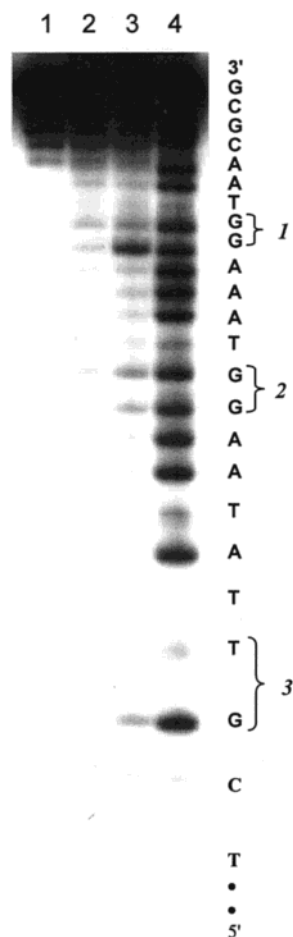


Figure 4. Autoradiogram depicting the photocleavage of DNA(4). All lanes are piperidine treated. Lane 1: DNA(4)/AQ-Og12, dark control; lane 2: DNA(4)/Og12, light control (60 min); lane 3: DNA(4)/AQ-Og12, (60 min); lane 4: Maxam–Gilbert A+G sequencing. DNA-(4) is ^{32}P 5'-end labeled.

Figure 5 where the cleavage efficiency at GG₁ is used as the standard for calibration. These data reveal essentially no difference in the relative strand cleavage efficiency at GG₂ and GG₃ for compounds containing either DNA(1) or DNA(5). This finding shows that migration of the radical cation in single-stranded DNA is not strongly dependent on base sequence between the GG steps.

A trap (low-oxidation potential site) might inhibit radical cation migration if it is placed before a GG step and if the radical cation must pass through the trap. This behavior is seen in duplex DNA when an 8-OxoG is substituted for a guanine.^{7,42} Saito and co-workers calculated ionization potentials (IP) for a series of DNA sequences and report that G-triplets have lower IP than GG steps.⁴³ We examined the photochemistry of AQ-Og12/DNA(6) to probe the ability of a G-triplet at G₂ to inhibit reaction at G₃. The results, shown schematically in Figure 5, reveal that the G-triplet actually enhances cleavage at G₃. About one-third more cleavage is observed at both sites when 3'-TGG₂-5' of DNA(1) is mutated to 3'-GGG₂-5' in DNA(6). This finding points to a special relationship between the two GG steps in the single-strand overhang of DNA(1).

We carried out two sets of experiments to probe the relationship between GG₂ and GG₃. In DNA(1), the first GG

step in the single-strand overhang region is only one base from the termination of the duplex region. We suspected that moving GG₂ farther from the duplex might reduce the efficiency of radical cation transfer from the duplex into the single-strand region. The single T between the duplex region and GG₂ is replaced by TAT in DNA(7). Figure 5 shows the results of irradiating AQ-Og12/DNA(7). Not only is the cleavage efficiency reduced at GG₂, but there is a corresponding reduction in reaction efficiency at GG₃ as well. This finding also points to a very close connection between the reactions at GG₂ and GG₃. We prepared and examined DNA(8) as the final step in probing this connection.

In DNA(8), the GG₂ sequence of DNA(1) has been replaced with 5'-TA-3' so that the only GG step in the single-strand region is GG₃. The results of irradiation of AQ-Og12/DNA(8) are shown in Figure 6. Comparison of these findings with those obtained from irradiation of AQ-Og12/DNA(1), Figure 2, is very revealing. GG₁, located in the duplex region, shows the expected 5'-selective cleavage in both cases, but the replacement of GG₂ with AT in DNA(8) inhibits reaction at GG₃ (lane 2, Figure 6). However, irradiation of the three-part hybrid [AQ-Og12+DNA-(8c)]/DNA(8), where GG₂ is replaced with 5'-TA-3' but GG₃ is part of a duplex, reveals 5'-G selective cleavage at GG₃ (lane 4, Figure 6). These results show convincingly that cleavage at GG₃ in single-stranded DNA requires GG₂. This finding, when combined with the results from other compounds described above, points to a mechanism for radical cation migration in single-stranded DNA that requires direct contact between remote guanines.

(4) Products Formed from Guanine Radical Cation.

Although an ultimate outcome is strand cleavage, there is considerable evidence showing that the initial reaction of a guanine radical cation as a free nucleotide or in single-stranded DNA is different from that which occurs in duplex DNA.^{24,26,44} The structure of AQ-Og12/DNA(1), with its clearly defined GG-containing duplex and single-strand regions, permits a careful assessment of guanine radical cation reactivity. We applied the method developed by Spassky and Angelov⁴⁴ to quantitate 8-OxoG formation based on the relative amount of strand cleavage induced by treatment with alkali or with Fpg. Fundamentally, piperidine treatment does not give strand cleavage at 8-OxoG,^{45,46} but Fpg does.⁴⁷ Thus, the difference between the cleavage yield observed for treatment of irradiated samples with Fpg or with piperidine is a measure of 8-OxoG formation.

Figure 7 shows schematically the results from irradiation of AQ-Og12/DNA(1). After irradiation DNA(1) was hybridized with DNA(2), its full complement, and then treated with either piperidine or Fpg. Clearly, reaction with Fpg gives significantly more cleavage at the 5'-G of GG₁, located in the duplex region, than does piperidine, whereas 3' and 5'-cleavage is nearly the same for GG₃ (located in the single-strand region) with piperidine and Fpg. These results are consistent with the conclusion that guanine radical cations in duplex DNA react with H₂O to form 8-OxoG. A guanine radical cation in the single-strand region may react with H₂O, but it also can lose a proton to give the guanine radical, which is trapped by O₂. These findings are in contrast to the recent claim that guanine radical cations at GG steps in duplex DNA give equal amounts of 5'- and 3'-reaction forming 8-OxoG only as a minor product.²⁹

(44) Spassky, A.; Angelov, D. *Biochemistry* **1997**, *36*, 6571–6576.

(45) Cullis, P. M.; Malone, M. E.; Merson-Davies, L. A. *J. Am. Chem. Soc.* **1996**, *118*, 2775–2781.

(46) Muller, J. G.; Duarte, V.; Hickerson, R. P.; Burrows, C. J. *Nucleic Acids Res.* **1998**, *26*, 2247–2249.

(47) David, S. S.; Williams, S. D. *Chem. Rev.* **1998**, *98*, 1221–1261.

(42) Ly, D.; Sanni, L.; Schuster, G. B. *J. Am. Chem. Soc.* **1999**, *121*, 9400–9410.

(43) Saito, I.; Nakamura, T.; Nakatani, K.; Yoshioka, Y.; Yamaguchi, K.; Sugiyama, H. *J. Am. Chem. Soc.* **1998**, *120*, 12686–12687.

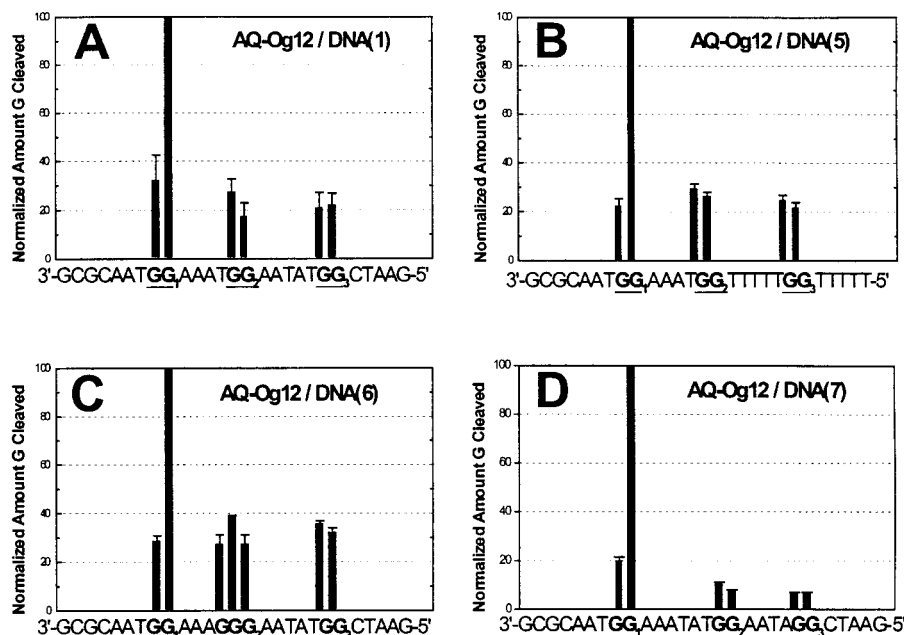


Figure 5. Schematic illustration of amount of G cleaved at all three GC steps in the duplex DNAs with dangling single strand. The values associated with each G were quantified and averaged from four separate experiments (represented by a solid column). The bars on the top of each column symbolize the standard deviations. (A) AQ-Og12/DNA(1); (B) AQ-Og12/DNA(5); (C) AQ-Og12/DNA(6); (D) AQ-Og12/DNA(7).

Discussion

The migration of radical cations in duplex DNA has been extensively investigated. One defining characteristic of this process is selective reaction at the 5'-G of GG steps. A second, more recently documented, characteristic is surprisingly shallow distance dependence for reaction efficiency that is more or less independent of specific sequence.^{17,18} We have attributed this behavior to a mechanism described as phonon-assisted polaron-like hopping. According to this proposal, the radical cation generates a local distortion of the duplex in order to relieve its electron deficiency. The radical cation is delocalized over the local distortion, and the distortion migrates by an activated process, which competes with its irreversible consumption. We suggest that the charge injected at the AQ-containing end of AQ-Og12/DNA(1), and related compounds studied here, migrates through the duplex region by this process.

Our results demonstrate that charge can also be transported in the single-stranded DNA region. However, it is also clear that the mechanism of transport in the single strand differs from the proposed migration mechanism for duplex DNA. This is revealed by the experiments described above. Most telling is the observation that reaction at GG₃ requires the presence of GG₂ in single-strand but not in duplex DNA.

Charge transport from the duplex region to GG₂ and to GG₃ may occur according to several different mechanisms. Kool and co-workers³⁰ have shown that the nucleotides in a "dangling" position (i.e., without a pairing partner) at the end of a base-paired duplex still maintain significant π -electron interaction with the duplex through end-capping. And, not surprisingly, due to their larger size purines end-cap more strongly than do pyrimidines. On this basis, we propose that radical cation transport to GG₂ occurs by its direct contact with the duplex. Two observations support this proposal. First, examination of DNA(7) shows that the reaction efficiency decreases when the number of nucleotides between the duplex and GG₂ increases. Second, conversion of the T adjacent to the duplex in DNA(1) to a G in DNA(6) increases the reaction efficiency at GG₂. We

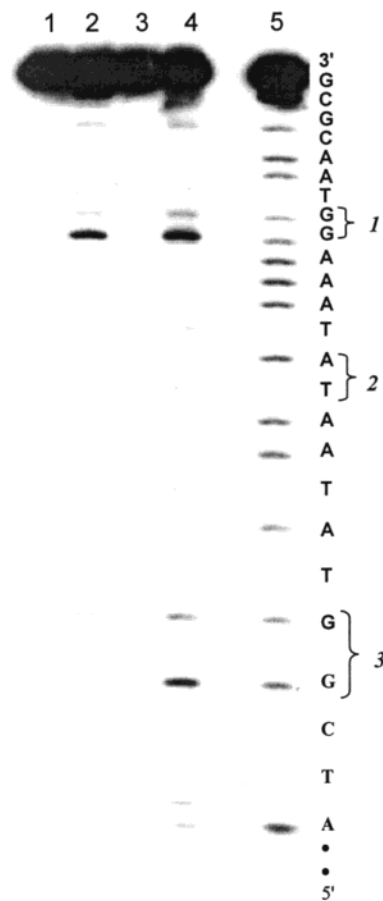


Figure 6. Autoradiogram depicting the photocleavage of DNA(8). All lanes are piperidine treated. Lane 1: DNA(8)/Og12, light control; lane 2: DNA(8)/AQ-Og12, (60 min); lane 3: DNA(8)/[Og12+DNA(8c)], light control; lane 4: DNA(8)/[Og12+DNA(8c)], (60 min); lane 5: Maxam-Gilbert A+G sequencing. DNA(8) is ³²P 5'-end labeled.

attribute this to stronger end-capping of the purine. Charge transport to GG₃ is a more complex matter because of the very

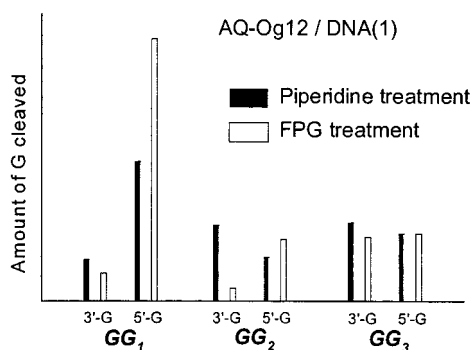


Figure 7. Schematic comparison of relative amounts of Fpg-labile and piperidine-labile products from irradiation of AQ-Og12/DNA(1).

large number of possible structures for single-stranded DNA. We consider three mechanistic possibilities.

The first mechanism we consider for charge transport to GG₃ parallels that proposed for the duplex DNA. In this case, sequential migration from one base to the next occurs when motions of the disordered single strand bring an electron acceptor and donor into proper juxtaposition. This possibility may be ruled out on several grounds. Base radical cations (the acceptors) are much more acidic than their neutral counterparts and, at the pH of these experiments, those that are exposed to solvent will lose a proton.^{48,49} There is no known mechanism for rapid migration of the base radical (deprotonated radical cation) along the DNA strand. Second, isolated guanines are approximately as likely to react as GG steps and GGG triplets, and there is no position preference in the latter two cases. If there were some sort of cooperative stacking along the radical cation-containing single strand, then the number of contiguous guanines should affect reaction efficiency and the particular G that reacts. Also, substitution of the triplet GGG₂ for GG₂ increases the cleavage efficiency at the “more distant” GG₃. This seems contrary to what should be observed if the radical cation had to pass through GGG₂ to get to GG₃. Finally, only for the single strand does removal of GG₂ inhibit reaction at GG₃. This suggests a special role for GG₂ in transporting the charge to GG₃.

The remaining two mechanistic possibilities we consider share the postulated formation of structures that bring the radical cation in close contact with one of the guanines located at GG₃. In principle, such a reactive structure could be formed by motions of the disordered single strand after the radical cation is injected, or it may be that reactive conformations existing in the ensemble of structures when charge injection occurs lead to reaction. We favor the latter because of competition with proton loss by the base radical cation in the single strand.

One set of structures to be considered are triplexes formed between appropriate base pairs of the duplex by folding back the single strand. For example, base triples such as with CG⊗G and TA⊗T (where ⊗ refers to Hoogsteen hydrogen bonding) are stable and readily characterized under appropriate conditions.⁵⁰ These structures are unstable at the low monovalent salt concentration used in this study. Nevertheless, they may exist at some low steady-state concentration and thus provide a means for radical cation migration from the duplex to GG₃ by direct contact. Two observations argue against this mechanism. First, substitution of the five bases between GG₂ and GG₃ in DNA-(1) with (T)₅ in DNA(5) should facilitate the formation of this

type of transient structure with the possible formation of two CG⊗G and three TA⊗T triplexes. However, DNA(1) and DNA-(5) give essentially the same reaction efficiency at GG₃. Second, the replacement of GG₂ by AT in DNA(8) should not greatly change triplex formation, but it does essentially eliminate reaction at GG₃.

A second possible set of reactive structures involves various non-Watson–Crick base pairings in the single-strand region. In particular, association of GG₃ and GG₂ provides an obvious route for charge migration to GG₃. It is well-known that purines, especially guanine, can pair with another purine base to form purine–purine “mispairs” through their available hydrogen-bond donors and acceptors.⁵¹ Several observations suggest that this type of structure plays the key role in charge transport to GG₃. Clearly, if GG₂ is not present, there can be no association, and the removal of GG₂ in DNA(8) stops reaction at GG₃. Also, the probability that there will be a GG mispair increases with the number of guanines. Thus, the purine mispair proposal is supported by the examination of DNA(6), which shows that conversion of GG₂ to GGG₂ increases the reaction efficiency at GG₃. The formation and reaction from GG mispairs also accommodates the approximately equal reactivity of GG₂ and GG₃ in DNA(1), if structures with this grouping are represented heavily in the population. Ultimately, of course, it is not possible to be definitive about the precise nature of the ill-defined structures in the single-stranded region based on relative reactivity data. Nevertheless, the evidence is consistent with the suggestion that radical cation transport in single-stranded DNA proceeds from guanine to guanine by direct contact in GG mispairs.

Conclusions

Our findings show that radical cations injected into duplex DNA can migrate into a single-strand overhang region. Radical cations in single-strand DNA react at guanines. This reaction is revealed as strand cleavage by subsequent treatment with piperidine or Fpg. The relative amounts of cleavage observed shows that 8-OxoG is a major product formed from reaction of guanine radical cations in duplex DNA. In contrast to radical cation reactions in duplex DNA, isolated guanines are as reactive as GG steps in single strands. Further, the characteristic 5'-G selective reaction at GG steps in duplexes is absent in single strands. This is attributed to the change from a well-ordered duplex structure having limited water access and stabilizing the radical cation on the 5'-G^{28,52} to a solvent-exposed, coiled single strand. The mechanism for radical cation transport in single-strand DNA is different from that found in duplex structures. We postulate that reactive structures resulting from GG mispairs bring remote guanines into close contact and that charge transport in single-strand DNA occurs from G to G in these structures.

Experimental Section

Materials and Instrumentation. Radioactive isotopes [γ -³²P]ATP were purchased from Amersham Bioscience. T4 Polynucleotide Kinase was purchased from Pharmacia Biotech and stored at -20 °C. Unmodified oligonucleotides (gel filtration grade) were obtained from the Midland Certified Reagent Company. 5'-End-linked anthraquinone oligonucleotides were synthesized as described elsewhere on an Applied Biosystems DNA synthesizer and were purified by reverse-phase HPLC.⁷ The extinction coefficients of the unmodified oligonucleotide were calculated using the nearest-neighbor values, and the absorbance

(48) Steenken, S. *Biol. Chem.* **1997**, *378*, 1293–1297.

(49) Steenken, S. *Free Radical Res. Commun.* **1992**, *16*, 349–379.

(50) Frank-Kamenetskii, M. D.; Mirkin, S. M. *Annu. Rev. Biochem.* **1995**, *64*, 65–95.

(51) Chou, S. H.; Zhu, L.; Reid, B. R. *J. Mol. Biol.* **1997**, *267*, 1055–1067.

(52) Prat, F.; Houk, K. N.; Foote, C. S. *J. Am. Chem. Soc.* **1998**.

was measured at 260 nm. Anthraquinone-modified oligonucleotide solution concentrations were determined the same way as that of the unmodified oligomers except that an anthraquinone was replaced with adenine in the extinction coefficient determination. Ion-exchange and reverse-phase HPLC were performed on a Hitachi system using a Vydac column. Matrix-assisted laser desorption ionization time-of-flight mass (MALDI-TOF) spectrometry of the conjugate strands was performed at the Midland Certified Reagent Company. All oligonucleotides gave the expected mass spectrum. The buffer solution used in all DNA experiments was 10 mM sodium phosphate at pH = 7.0. UV melting and cooling curves were recorded on a Cary 1E spectrophotometer equipped with a multicell block, temperature controller, and sample transport accessory.

Thermal Denaturation. Samples were prepared consisting of equimolar concentrations of DNA oligomers (4.0 μ M each) in 1 mL of 10 mM sodium phosphate buffer (pH 7.0). Samples were placed in cuvettes (1.5 mL capacity, 1.0 cm path length) and sealed with tape to prevent evaporation of water during heating/cooling cycles. The absorbance of the samples at 260 nm was monitored as a function of temperature for three consecutive runs: heating 1.0 $^{\circ}$ C/min, then cooling followed by reheating at 0.5 $^{\circ}$ C/min.

Cleavage Analysis by Radiolabeling and PAGE. DNA oligonucleotides were radiolabeled at the 5'-end. 5'-OH labeling involved the use of [γ - 32 P]ATP and bacterial T4 Polynucleotide kinase. The labeling was performed according to standard procedures. Radiolabeled DNA was purified by 20% PAGE. Samples for irradiation were prepared by hybridizing a mixture of "cold" and radiolabeled oligonucleotide (4 μ M) to a total volume of 10 μ L each in 10 mM sodium

phosphate, pH = 7.0. Hybridization was achieved by heating the samples at 90 $^{\circ}$ C for 5 min, followed by slow cooling to room temperature over the course of 3 h. Samples were irradiated in microcentrifuge tubes in a Rayonet photoreactor (Southern New England Ultraviolet Company, Barnsford, CT) equipped with 8 \times 350 nm lamps at 20 $^{\circ}$ C. After irradiation, the samples were precipitated once with cold ethanol in the presence of glycogen, dried, and treated with 1 M piperidine at 90 $^{\circ}$ C for 30 min. After evaporation of the piperidine, drying, and suspension in denaturing loading buffer, the samples (1500 cpm) were electrophoresed on a 20% 19:1 acrylamide:bis-acrylamide gel containing 7 M urea. The gels were dried, and the cleavage sites were visualized by autoradiography. Quantification of cleavage bands was performed on a phosphorimager.

Fpg Treatment. After the irradiation, the standard reaction mixture (10 μ L) prepared according to the previous procedure was mixed with an excess of its "full" complementary strand and incubated at 90 $^{\circ}$ C for 5 min followed by slowly cooling to room temperature. The resulting solution was adjusted to contain 50 mM Tris \cdot HCl (pH 7.5), 2 mM EDTA, 70 mM NaCl, and 10 μ g of Fpg and incubated at 37 $^{\circ}$ C for 30 min. Reactions were terminated by heating at 70 $^{\circ}$ C followed by ethanol precipitation at -20 $^{\circ}$ C. The reaction mixture was analyzed by 20% PAGE containing 7 M urea.

Acknowledgment. This work was supported by grants from the NIH and NSF for which we are grateful.

JA992224R